# SPLIT HIGHER ORDER MODES IN SUPERCONDUCTING CAVITIES*

H. Hahn ◊, S. Belomestnykh, Wencan Xu, BNL, Upton, NY 11973, USA

*Abstract*

Split resonances are a common appearance in superconducting cavities and are studied here on the specific examples of the TE11 and TM11- like dipole resonances in five-cell copper models of the Brookhaven ERL and BNL3 cavities. The BNL3 was designed to be suitable for the envisioned high-intensity projects at this laboratory. Achieving the required high current performance depends on avoiding beam-breakup instabilities by minimizing the Higher Order Modes (HOM) *Q*-values. This was attempted in the design phase and will be done with appropriate mode dampers in operation. The availability of a copper model provided the convenient opportunity to confirm the design and to study potentially nefarious high-*Q* resonances. The appearance of split resonances impeded the HOM identification and the theoretical interpretation as ellipticity deformation is presented in this paper.

## INTRODUCTION

Improvements of RHIC operation will depend to a large degree on the application of superconductivity (SC) to RF cavities. Intrinsic to all SC cavities is the appearance of higher order modes and the permanent need of their study. The splitting of resonance frequencies is a specific problem, complicating the HOM mode identification and preventing reliable *Q*-measurements. The splitting is found already in normal conducting (NC) cavities and can be conveniently performed on the Niobium cavity of the Energy Recovery Linac (ERL) [1] or the copper cavity model for the BNL3 cavity [2] shown in Fig. 1. The BNL3 was designed to be suitable for the envisioned high-intensity projects at this laboratory, and experimentally confirming the design assumptions is mandated. Significant frequency deviations from the design values are expected due to beam tube end effects. The small resonance frequency splitting is here explained, using Mathieu functions, as fabrication-caused ellipticity deformation.

## BNL3 DIPOLE RESONANCES

Cavity resonances are obtained from $S_{21}$ transmission measurements with a network analyzer (NA) [3]. BNL3 cavity has simple type-N connectors used as probes in cell 1 and 2 together with stronger coupling fundamental power coupler (FPC) and pickup (PU) probes. Figure 2 shows the transmission in the first dipole pass band through the cavity from cell 1 to 5 and across from FPC to PU. Note the repetitive resonances in the signal across the cavity, presumably due to the tapered end tubes. Not explained is a stop pass filtering in the central range.

The cavity resonances are seen in both scans, although the cell run has a single non-split resonance at ~935 MHz with the highest measured *Q*, next to the split one at 932.3 MHz. Table I lists the identified split dipole modes.

Table 1: Dipole Resonances

| $f_{even}$ | $f_{odd}$ | $\Delta\times10^4$ |
|---|---|---|
| 821.26 | 821.78 | 6 |
| 827.25 | 828.09 | 10 |
| 843.5 | 844.29 | 9 |
| 866.13 | 867.10 | 11 |
| 885.91 | 886.47 | 6 |
| 906.7 | ~ | |
| 932.31 | ~ | |
| 954.17 | 954.48 | 3 |
| 987.90 | 988.05 | 1 |
| 1007.03 | 1007.16 | 1 |
| 1016.78 | 1016.94 | 1 |
| 1020.95 | 1021.03 | <1 |


Figure 1: BNL3 Copper cavity.

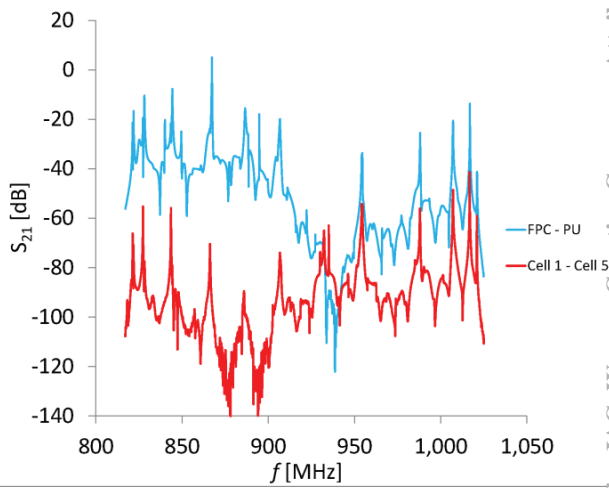


Figure 2: Frequency scan across BNL3,

◊ hahnh@bnl.gov

*Work supported by Brookhaven Science Associates, LLC under contract no. DE-AC02-98CH10886 with the DOE.




ISBN 978-3-95450-122-9

*Split Dipole Resonances at 821 MHz*

The lowest dipole resonance at 821 MHz represents the prototypical split HOM and was fully measured with different excitations as shown in Fig. 3. The highest $Q$ value obtained is 21,300, essentially independent of the probe combinations. The signal strength of the lower-$f$ "even" mode is larger with horizontally placed probes pointing to a prolate cavity deformation. A theoretical underpinning of the mode features are given in the next section.

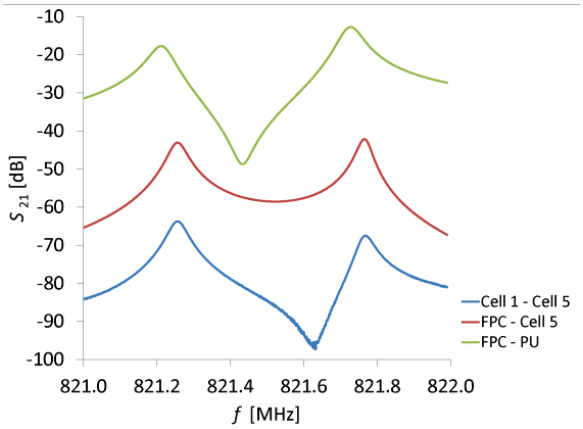


Figure 3: $S_{21}$ transmission at 821 MHz.

## ANALYSIS VIA MATHIEU FUNCTIONS

It can be to assume that the resonance splitting is caused by deforming a perfectly cylindrical tube/cavity into a prolate ellipse with the major axis, $a$, and the minor axis, $b$. The deformation is characterized by an eccentricity, $\varepsilon = \sqrt{1-(b/a)^2}$ or in terms of the focal length, $h = \varepsilon a$. The deformation retains the perimeter, and is found as $P = 4aE(\varepsilon^2)$ with $E(\varepsilon^2)$ the complete elliptic integral of the second kind. Electromagnetic fields are solved in elliptic cylinder coordinates ( $\xi, \eta, z$ ) related to Cartesian coordinates ( $x, y, z$ ) by

$$x = h\cosh\xi\cos\eta\,,\; y = h\sinh\xi\sin\eta \qquad (1)$$

The surface $\xi =$ constant is a cylinder of elliptic cross section and $\eta =$ constant is a hyperbolic cylinder of two sheets with foci at $(\pm h, 0)$. The wall of the elliptic cylinder defines $\xi_0$ from $a = h\cosh\xi_0$ or $\varepsilon\cosh\xi_0 = 1$. The correlation of the elliptic cylinder with the cylindrical polar, $(r, \varphi)$, coordinates is complex but the simple relation of $\tan\varphi = \sqrt{1-\varepsilon^2}\tan\eta$ is useful in the limit of small excentricity.

The field components for TE and TM time harmonic waves, are derived from scalar potentials written as the product of Mathieu functions [4],

$$u_{even} \propto Ce_m(q,\xi)ce_m(q,\eta)\,,\; u_{odd} \propto Se_m(q,\xi)se_m(q,\eta) \qquad (2)$$

with solutions of the coupled canonical and the modified (radial) Mathieu differential equations

$$\frac{\partial^2}{\partial\eta^2}\begin{Bmatrix} ce_m(\eta,q) \\ se_m(\mu,q)\end{Bmatrix} + \left(\begin{Bmatrix} a_m \\ b_m\end{Bmatrix} - 2q\cos 2\eta\right)\begin{Bmatrix} ce_m(\eta,q) \\ se_m(\eta,q)\end{Bmatrix} = 0 \qquad (3)$$

$$\frac{\partial^2}{\partial\xi^2}\begin{Bmatrix} Ce_m(\xi,q) \\ Se_m(\xi,q)\end{Bmatrix} - \left(\begin{Bmatrix} a_m \\ b_m\end{Bmatrix} - 2q\cosh 2\xi\right)\begin{Bmatrix} Ce_m(\xi,q) \\ Se_m(\xi,q)\end{Bmatrix} = 0$$

where $a_m$ and $b_m$ are the even and odd characteristic values and

$$q = \frac{1}{4}h^2(k^2 - k_z^2)\,,\; k = \omega/c \text{ and } k_z = 0 \text{ at cutoff.} \qquad (4)$$

The time harmonic electric field components, $e^{j\omega t}$, on the wall of the $TE_{11}$ mode are found as

$$E_\xi = \frac{Ce_1(\xi_0, q_{TE11})se_1'(\eta, q_{TE11})}{\sqrt{1-(h/a)^2\cos^2\eta}}$$

$$E_\xi = \frac{C'e_1(\xi_0, q_{TE11})se_1(\eta, q_{TE11})}{\sqrt{1-(h/a)^2\cos^2\eta}} \qquad (5)$$

Assuming the use of electric probes for the $S_{21}$ transmission measurements, the coupled $TE_{11}$ field components on the wall boundary of an elliptical structure are approximated by an even and an odd function,[5,6]

$$u_e \propto \frac{J_1(2\sqrt{q}\cosh\xi_0)}{\sqrt{1-q^2\cos^2(\eta-\psi)}}\left[\cos(\eta-\psi) - (q/8)\cos 3(\eta-\psi) + \ldots\right]$$

$$u_o \propto \frac{J_1(2\sqrt{q}\cosh\xi_0)}{\sqrt{1-q^2\cos^2(\eta-\psi)}}\left[\sin(\eta-\psi) - (q/8)\sin 3(\eta-\psi) + \ldots\right]$$

where $\eta \approx \varphi$ is the angular probe position, and $\psi$ is the excitation angle versus the major axis in a prolate cavity. In first approximation, the ε-dependent $q$-parameter is given by the $TE_{11}$ cutoff frequency via $\varepsilon = 1/\cosh\xi_0$ as $2\sqrt{q}/\varepsilon = j_{11}'$, solution of the Bessel function, $J_1'(j_{11}') = 0$ and $j_{11}' \simeq 1.8412$, yielding the ratio of cutoff wavelength to the perfect tube radius as $\lambda_{co}/a \simeq 3.4126$.

In contrast to the minimal effect of a small eccentricity on field shape, the cut-off frequencies are noticeably split into even and odd solutions with their ratio of wave length to radius defined in the literature as

$$\frac{\lambda_{co}}{a} = \frac{\pi\varepsilon}{\sqrt{q}} \qquad (7)$$

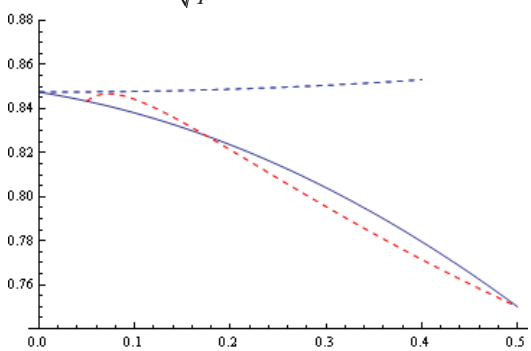


Figure 4: Characteristic values of $TE_{11}$ mode, even dotted blue, odd dotted red, and fitted odd solid, respectively.

The $TE_{11}$ $q$-values have been obtained numerically by Kretschmar as [7]

$$q_{CTE11} \simeq 0.8476\varepsilon^2 - 0.0013\varepsilon^3 + 0.0379\varepsilon^4$$

$$q_{STE11} \simeq -0.0018\varepsilon + 0.8974\varepsilon^2 - 0.3679\varepsilon^3 + 0.1612\varepsilon^4 . \quad (8)$$

The interesting range of $\varepsilon \to 0$ is obtained by fitting the available numerical results in Eq. 8 to the circular tube with $\lim_{\delta\varepsilon\to 0} q_{S11}/\varepsilon^2 = 0.8475$, yielding

$$q^{\diamond}_{STE11} \approx 0.8475\varepsilon^2 - 0.0888\varepsilon^3 - 0.2118\varepsilon^4 \quad (9)$$

Fig. 4 shows the characteristic values for the $TE_{11}$ mode over the interesting $\varepsilon$ range. The odd $q_{S11}$ (dotted red) and (solid) $q^{\diamond}_{S11}$ from $0.05 \le \varepsilon \ge 0.5$ confirm a good fit.

For comparison, the wave propagation for $TM_{11}$ follows from $j_{11} = 3.8317$ and has the $\lambda_{co}/a \simeq 1.6398$ in the round wave guide. The characteristic values for the $TM_{11}$ values were fitted (super script $\diamond$) over the available range in [7] yielding

$$q^{\diamond}_{CTM11} \simeq 3.6705\varepsilon^2 - 0.1140\varepsilon^3 + 1.4862\varepsilon^4$$

$$q^{\diamond}_{STM11} \simeq 3.6705\varepsilon^2 - 0.2084\varepsilon^3 + 3.8901\varepsilon^4 \quad (10)$$

### *Frequency Splitting*

Whereas the field shape is minimally affected by the ellipticity, the cutoff frequencies are split yielding the numerical expressions for their ratio [8]

$$\Delta(\lambda_{CTE}/\lambda_{STE}) \simeq 0.1032\varepsilon + 0.3054\varepsilon^2$$

$$\Delta(\lambda_{CTM}/\lambda_{STM}) \simeq 0.0129\varepsilon - 0.3268\varepsilon^2 \quad (11)$$

The measured $TE_{11}$ frequency deviation at ~821 MHz of $\Delta \approx 6\times10^{-4}$ yield the numerical $\varepsilon = 0.0057$ and the focal distance $h = \varepsilon a \approx 0.3$ mm, similar to TESLA results [9].

## CONCLUDING SIMULATION

The $S_{21}$ transmission across the split 821 MHz dipole resonance is shown in Fig. 3 above. It led to the assumption that the intrinsic $Q$ value is constant. Allowing in addition that the excitation of the modes with the coupling, $\kappa$, is done with equal probes at in and output and occurs in the same plane, defined by $\Upsilon = \eta - \psi$. The measured transmission can then be simulated according to Eq. 12,

$$S_{21} = \kappa\cos\Upsilon / \left\{1 + jQ\left(\frac{\omega}{\omega_e} - \frac{\omega_e}{\omega}\right)\right\} + \kappa\sin\Upsilon / \left\{1 + jQ\left(\frac{\omega}{\omega_o} - \frac{\omega_o}{\omega}\right)\right\}$$

with the measured split frequencies, $\omega_e, \omega_o$, while $Q, \kappa$ and $\Upsilon$ are estimated or used as free fitting parameters. The highest $Q$ $TM_{11}$ mode at ~1021 MHz is simulated in Mathematica with $Q \approx 43{,}000$ and its $S_{21}$ is shown in Fig. 5 on top, confirming the validity of the model, excitation through equal κ to the split modes, although changing with the probe plane positions. The splitting is caused by the two mode polarizations with $\Upsilon \approx 10°$ (blue) and 75° (red).

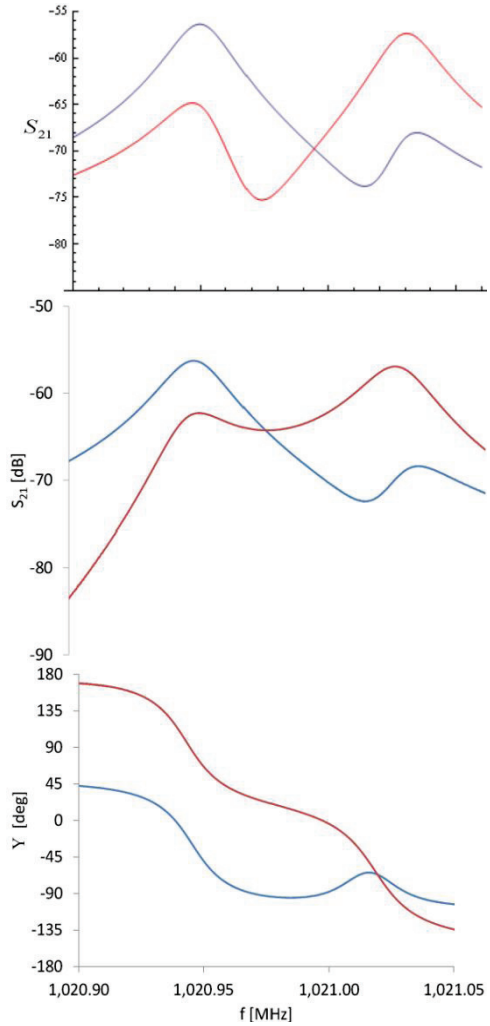


Figure 5: Simulated and measured $S_{21}(f)$ scans at 1021 MHz between cell 1and 5 (blue) and cell 1 to PU (red).

## REFERENCES

[1] H. Hahn, I. Ben-Zvi, L. Hammons, E.C. Johnson, J. Kewisch, V. N. Litvinenko, Wencan Xu, Phys. Rev. ST Accel. Beams **13**,121002 (2010) .

[2] Wencan Xu, I. Ben-Zvi, R. Calaga, H. Hahn, E.C. Johnson, J. Kewisch, Nucl. Instr. Methods, Phys. Research A (2010), doi: 10.1016/j.nima.2010.06.245.

[3] H. Hahn, R. Calaga, Puneet Jain, E.C. Johnson, Wencan Xu, Nucl. Instr. Methods, Phys. Research A, doi: 10.1016/j.nima.2012.

[4] N. Marcuvitz, Waveguide Handbook, (McGraw Hill Book Co, Inc,1951) p. 80.

[5] D.A. Goldberg, L. J. Laslett, R. A. Rimmer, Report LBL-28702.

[6] G. Blanche in M. Abramowitz and I. A. Stegun, Handbook of Mathematical Functions (1966) p. 721.

[7] J. Kretzschmar, IEEE Trans. MTT-18, No. 9, (1970), p. 547.

[8] Wencan Xu, S. Belomestnykh, I. Ben-Zvi, H. Hahn, Report BNL-08926-2012-IR, C-A/AP/#472 (2012).

[9] A. Leblanc, TESLA Report 2007-1 (2007).




ISBN 978-3-95450-122-9